Three-dimensional reconstruction of rat knee joint using episcopic fluorescence image capture.

AUTHOR(S):

Takaishi, R; Aoyama, T; Zhang, X; Higuchi, S; Yamada, S; Takakuwa, T

CITATION:

Takaishi, R ...[et al]. Three-dimensional reconstruction of rat knee joint using episcopic fluorescence image capture.. Osteoarthritis and cartilage 2014, 22(10): 1401-1409

ISSUE DATE:

2014-10

URL:

http://hdl.handle.net/2433/191262

Three-dimensional reconstruction of rat knee joint using episcopic fluorescence image capture

Ryota Takaishi,[1] Tomoki Aoyama,[1] Xiangkai Zhang,[1] Shinya Higuchi,[1] Shigehito Yamada,[1,2] and Tetsuya Takakuwa[1]

[1]Human Health Science, Graduate School of Medicine, Kyoto University, Kyoto, Japan

[2]Congenital Anomaly Research Center, Graduate School of Medicine, Kyoto University, Kyoto, Japan

E-mail addresses:

RT: lshl.tr@gmail.com

TA: blue@hs.med.kyoto-u.ac.jp

XZ: zhang.xiangkai.48v@st.kyoto-u.ac.jp

SH: tpshinya@gmail.com

SY: shyamada@cac.med.kyoto-u.ac.jp

TT: tez@hs.med.kyoto-u.ac.jp

Address correspondence to: T. Aoyama

Human Health Sciences, Graduate School of Medicine, Kyoto University

53 Kawahara-cho, Shogoin, Sakyo-ku, Kyoto 606-8507, Japan

E-mail: blue@hs.med.kyoto-u.ac.jp

Phone: +81-75-751-3952

Abstract

Objective: Development of the knee joint was morphologically investigated, and the process of cavitation was analyzed by using episcopic fluorescence image capture (EFIC) to create spatial and temporal three-dimensional (3D) reconstructions.

Methods: Knee joints of Wister rat embryos between embryonic day (E)14 and E20 were investigated. Samples were sectioned and visualized using an EFIC. Then, two-dimensional image stacks were reconstructed using Osirix software, and 3D reconstructions were generated using Amira software.

Results: Cavitations of the knee joint were constructed from five divided portions. Cavity formation initiated at multiple sites at E17; among them, the femoropatellar cavity was the first. Cavitations of the medial side preceded those of the lateral side. Each cavity connected at E20 when cavitations around the anterior and posterior cruciate ligaments were completed.

Conclusion: Cavity formation initiated from six portions. In each portion, development proceeded asymmetrically. These results concerning anatomical development of the knee joint using EFIC contribute to a better understanding of the structural feature of the knee joint.

Keywords: episcopic fluorescence image capture, knee joint, joint cavity, development

Running title: 3D reconstruction of the knee joint

Abbreviations:

femoropatellar cavity (FPC), medial femoromeniscal cavity (mFMC), lateral femoromeniscal cavity (lFMC), medial meniscotibial cavity (mMTC), lateral meniscotibial cavity (lMTC), circumligament cavity (CLC), anterior cruciate ligament (ACL), posterior cruciate ligament (PCL), medial meniscus (MM), lateral meniscus

(LM), episcopic fluorescence image capture (EFIC), embryonic day (E), three-dimensional (3D), hematoxylin and eosin (H&E), confidence interval (CI)

Introduction

The synovial joint is a complex multi-tissued organ that is essential for skeletal function[1]. Synovial joints arise through two main processes. In long bone elements, cartilaginous differentiation occurs across the location of the prospective joint that then segments secondarily[1-3]. Cavitation of the joint follows, driven by selective high-level synthesis of hyaluronan by interzone cells and presumptive synovial cells[4]. This process has fascinated developmental biologists for decades[5-7].

The knee joint—one of the largest synovial joints—consists of distinct tissues including bones, articular cartilages, ligaments, synovial membrane, cruciate ligaments, menisci, and other components that interact to mechanically stabilize the joint and allow smooth motion[5]. The joint cavity of the knee is anatomically complicated and involves the space between the tibial plateaus, two femoral condyles, and the patella. The cavity is divided into at least five parts during the developmental stage, including the femoropatellar cavity (FPC), medial femoromeniscal cavity (mFMC), lateral femoromeniscal cavity (lFMC), medial meniscotibial cavity (mMTC), and lateral meniscotibial cavity (lMTC)[7].

The initiation, and spatial and temporal formation of the cavity is an important issue in joint development. Development of the joint cavity has been described in several different species, including rats[8] and humans[9]. However, the timing of cavity formation is ambiguous and discrepant, and the schedule of formation of the five parts has not been fully investigated. Ito and Kida reported that formation of the knee joint cavity in rats seemed to start at embryonic day (E)16.5 in paraffin-embedded sections, but that lacunal spaces were confirmed between spindle cells at E18.5 in resin-embedded sections[8]. Their study indicates that an artificial cleft during histologic preparation may interfere with the judgment of joint cavity formation.

Episcopic three-dimensional (3D) imaging involves novel techniques that create volume data by capturing images of subsequent surfaces of blocks containing histologically processed and embedded specimens during their physical

sectioning on microtomes. Such techniques have been used for creating 3D computer models in morphologic studies[10, 11]. Of the techniques, episcopic fluorescence image capture (EFIC)[12, 13] and high-resolution episcopic microscopy[14] have been successfully applied in recent research, while other applications, such as fast 3D serial reconstruction[15], surface imaging microscopy[16, 17], and serial block-face scanning electron microscopy[18], are not yet routine and only preliminary results are currently available.

EFIC was designed for analyzing the morphology of the organ systems of normal and malformed embryos[12-13, 19]. The specimens are embedded in a reddish-stained medium on a wax base. Then, monochrome light is applied to the block surface in order to excite autofluorence of the tissues. EFIC has higher image resolution than other 3D imaging modalities, such as magnetic resonance microscopy[12, 20-22], with fewer artifacts compared with conventional histologic methods. EFIC utilizes autofluorescent signal originating from pyridine nucleotides[12, 20], which exist in every cell of the body. High-intensity regions imply high cell density or high proliferation rate. The structural components of the knee during the prenatal period have been visualized, but never using EFIC. For example, with EFIC, the joint cavities may be clearly recognizable as low-density areas because they contain few cells.

In the present study, taking advantage of EFIC, development of the knee joint was morphologically investigated, and the process of cavitation was analyzed using spatial and temporal 3D reconstructions.

Materials and Methods

Animals

Fifty hindlimbs (25 right, 25 left) were removed from 25 white Wister rat embryos between E14 and E20, except for E15 (E14, n = 3; E16, n = 2; E17, 18, 19, 20, n = 5 each). Wister rats were obtained from SHIMIZU Laboratory Supplies Co., Ltd (Kyoto, Japan). All of the mother rats were sacrificed by pentobarbital sodium

overdose before caesarean section. Whole rat embryos were fixed immediately after removal from the uterus in 4% paraformaldehyde at 4°C overnight before dissecting the hindlimbs. Samples of the knee joint then were dehydrated in graded ethanol and xylene, according to conventional histologic processes.

Preparation and workflow for EFIC

Preparation of the samples for EFIC was performed as described elsewhere[12, 13, 19-21], with some modifications. Briefly, for EFIC, the dehydrated samples were infiltrated and embedded in 70.4% paraffin wax, containing 24.9% Vyber, 4.4% stearic acid, and 0.4% Sudan IV[21]. Incorporation of Sudan IV in the paraffin wax blocks fluorescence bleed-through from deeper layers of the tissue[20, 21]. The paraffin blocks were sectioned using a Leica SM2500 sliding microtome (Leica Microsystems, Bannockburn, UK) at 5-7 μm. Autofluorescence at the paraffin block face was visualized using epifluorescence imaging with mercury illumination and a discosoma Redfilter (excitation/emission of 545/620 nm, respectively). Fluorescent images were captured using a Hamamatsu ORCA-ER low-light CCD camera (HAMAMATSU Photonics K.K., Shizuoka, Japan). The resolution of the camera was 300 pixels/inch, and pixel size was 1344 × 1024 pixels. The field of view ranged between 2352 × 1792 μm and 5672 × 4321 μm. Digital images of the tissues on the surfaces of the blocks containing the specimens were captured with the camera sitting on a magnifying optic[10, 12, 13, 19-21]. The optical pathway of the optic was aligned precisely perpendicular to the block surface. After capturing an image of the block face, a small slice of the block was removed using the microtome blade. This slice permitted preservation of histologic sections for hematoxylin and eosin (H&E) staining. Then, a digital image of the freshly cut block surface was captured and the next slice of embedding block was removed. This procedure was repeated until the region of interest was sectioned and a stack of aligned digital images showing subsequent block faces with tissues

of the specimens was produced. Optical magnification ranged between ×25 and ×60, whereas the digital resolution ranged between 1.75 and 4.22 μm^2/pixel.

Analysis

Two-dimensional (2D) image stacks obtained by EFIC were reconstructed using Osirix 4.0 (Pixmeo SARL, Geneva, Switzerland). These 2D images were resectioned digitally to generate sagittal, transverse, and coronal sections. The parts of interest of the knee, such as cavity, ligament, and meniscus, were segmented on 2D serial sections manually and then reconstructed three-dimensionally without smoothing using AMIRA 5.4.0 software (Visage, Berlin, Germany). Manual segmentation of each lesion was performed by three individual researchers (RT, ZX, and HS), according to the criteria for that anatomic portion, and assessed by two individual observers (TA and TT). The results of segmentation were almost equal. Volume of the joint cavity was calculated as an integration of the area on 2D serial images using the same software.

Ethics

All of the experiments with animals were approved by the Institutional Animal Research Committee and performed according to the Guidelines for Animal Experiments of Kyoto University.

Statistical analysis

All data are shown as mean ± SD. The software program SPSS Statistics (IBM, Armonk, NY) was used for statistical analysis. Differences in volume between the femoropatellar cavity (FPC) and the other five cavities (described in the Results section) at each developmental stage was assessed using the Student's *t* test. Significant differences between the FPC and the other cavities at the same time interval were expressed using a length of the 95% confidence interval (CI). One-

way analysis of variance (ANOVA) and the Tukey-Kramer test were performed to examine differences in cavity volume among developmental stages.

Results

Comparison of EFIC and H&E staining

Major components of the knee joint were distinguishable as different signal intensities on EFIC after the E17 stage (Figure 1). The periosteum (Figure 1A) and ligaments (Figure 1A, asterisk) showed relatively high autofluorescent intensity due to dense distribution of the cells, whereas, cartilaginous anlagen showed lower autofluorescent intensity (Figure 1A). Each component of the knee joint was clearly distinguishable by its intensity according to the proceeding of development. The cavity had low intensity (Figure 1B, arrow), while the border of the cavity had high intensity (Figure 1B, arrowhead). In particular, just before cavity formation (Figure 1C [ii], arrowhead), the signal intensity of the border increased (Figure 1C [i], arrow).

Morphogenesis of the knee joint

Development of the knee joint cavity from E16 to E20 was precisely observed using EFIC and then analyzed with 3D reconstructions.

The structures of bone anlagen and interzone were not observed in the presumptive areas of limb bone formation in all three specimens at E14 (data not shown).

A low-intensity area corresponding to chondrification was observed in the femur, tibia, and fibula in the two specimens at E16 (Figure 2A). A three-layered structure corresponding to interzone also was seen between the femur and tibia in the two specimens at E16 (Figure 2B). First, we observed a couple of samples at each embryonic stage. However, the joint cavity was not observed before E16. Therefore, the sample number was added (n = 5) and quantification of the joint cavity was performed in the samples after E17.

The joint cavities were named based on position and place according to Gray's description[7]: femoropatellar cavity (FPC), medial femoromeniscal cavity (mFMC), lateral femoromeniscal cavity (lFMC), medial meniscotibial cavity (mMTC), lateral meniscotibial cavity (lMTC), and circumligament cavity (CLC). Analogues of the anterior cruciate ligament (ACL) and posterior cruciate ligament (PCL) were initially recognizable as faint lines with high intensity at E17 (Figure 3A [ii]). The lateral meniscus (LM) (Figure 3A [i]) and medial meniscus (MM) (Figure 3A [iii]) were recognizable as a high-intensity triangular shape connecting to the surface mesenchymal tissues at the joint. The patella was observed as a low-intensity area, whereas, the patellar ligament was seen as a relatively high-intensity area (Figure 1B [i], Figure 3A [ii]). The initial joint cavity formed simultaneously at the FPC, mFMC, and lFMC in 4 out of 5 specimens (Figure 3A, B). The FPC had a notch-like formation from both the cranial and caudal sides of the patella (Figure 1B [i], Figure 3A [ii]). The mFMC was observed as a large distinct cavity, while the lFMC was seen as several small dots. No cavities were observed around the ACL or PCL in the 5 specimens.

Initiation of cavitation at the mMTC and lMTC was detected for the first time in 3 out of 5 specimens at E18 (Figure 4A [iii]). The FPC and mFMC became large distinct cavities, but the lFMC was still small. A lining of high intensity around the cavity also was detected. At this stage, small cavities around the ACL and PCL were detected in 4 out of 5 specimens. This cavity could not be classified into the traditional five classifications (i.e., FPC, mFMC, lFMC, mMTC, and lMTC), so we named it the circumligament cavity (CLC).

Each component of the knee joint—femur, tibia, fibula, ligaments, and menisci—were well defined at E19 (Figure 5). The patella also was clearly differentiated, the ACL and PCL became sharp and thick, and the FPC became a large space. The mMTC and lMTC became large and connected with the mFMC and lFMC, respectively, in 3 out of 5 specimens. The cavities of the medial side were always larger than those of the lateral side. At this stage, the knee cavity was

separated into three parts since the cavities around the ACL and PCL were limited.

Autofluorescent intensity at both cruciate ligaments and the lining around the cavity increased, showing a contrast to other tissues, at E20 (Figure 6A). Although the cruciate ligaments were initially observed as an area of high intensity at E17 (Figure 3), they were clearly recognizable as mature constructs at E20 (Figure 6A [ii]). Cavitations around the ACL and PCL proceeded, connecting all cavities together.

Morphometry of cavity formation

The volume of the FPC and the other five cavities (mFMC, lFMC, mMTC, lMTC, and CMC) at each developmental stage was measured (Figure 7). The volume of the FPC increased significantly between E17 and E20 ($p = 0.002$), E18 and E20 ($p = 0.003$), and E19 and E20 ($p = 0.009$). The volume of the other five cavities also increased significantly between E17 and E20 ($p = 0.007$), E18 and E20 ($p = 0.009$), and E19 and E20 ($p = 0.047$). The volume of the FPC preceded that of the other cavities, but not to a significant degree (E17: 95% CI, -1.043-1.480; E18: 95% CI, -1.859-4.447; E19: 95% CI, -0.064-8.367; E20: 95% CI, -24.660-36.789).

Discussion

In the present study, the spatial and temporal process of knee joint cavity formation was described using EFIC and 3D reconstructions. The primary findings were as follows: Cavitation began from six portions, including the cranial and caudal sides of the FPC, mFMC, and lFMC, at E17. Cavitation of the MTC followed at E18. Cavitations of the medial side of the MTC preceded those of the lateral side. All cavities were connected at E20 when cavitations around the ACL and PCL were completed.

The EFIC system had several advantages in the present analysis. Joint cavities are mechanically fragile and prone to interference by artifacts during histologic preparation. In this regard, EFIC has a great advantage in that much

fewer artifacts are expected compared with conventional histologic methods[10, 12, 13, 19-22]. The firm embedded block was imaged and no staining was required in EFIC, whereas, thin sectioned samples were observed after staining in the conventional histologic method. In addition, joint cavities were clearly recognizable as very low–density areas in EFIC, as expected. High-intensity regions on EFIC images imply high cell density or high proliferative rate[12, 20]. In this point of view, it should be noted that the border of the cavity was highlighted as a linear structure with high intensity, indicating the presence of well-proliferating cell groups (Figure 1B, C). In histologic analysis, a single-layered cell was recognizable after E17 (Figure 1B [ii], arrowhead). The process of cavitation seems to be affected by multiple factors, including mechanical forces generated from muscle contraction[23], increase of hyaluronan and hyaluronan-binding protein synthesis[24, 25], and decrease of collagen fibrils in the interzone[8]. Ito and Kida reported that the mechanism of joint cavitation was based on proliferation and immigration of cells in the intermediate zone rather than apoptotic cell death[8]. Whether or not the cells at the high-intensity line are involved in the process of cavitation is subject to further study.

EFIC data may suggest the existence of a novel proliferative area, which had not been properly recognized before. Each component of the joint had changing signal intensity during development. The triangular area, which became the meniscus at later stages, was recognizable as an area of high intensity (Figure 1C [i], asterisk). A high-intensity area was detected at the peripheral area of the triangle facing the joint cavity (Figure 1C [i], arrowhead), demonstrating the initiation of joint cavity formation. This area later connected to the high-intensity lining at the border of the cavity. The migration of cells from the intermediate zone to around the cavity has been shown in a previous study[8]. The migrated cells may accumulate and increase the density of the cells, especially in the peripheral area of the triangle. The cruciate ligaments were another component in which the signal intensity gradually increased until E20. Usually, the cell density of the ligaments is low in adults. The kinetics of the cells in the ligaments during development is

variable and worth studying.

The formation of suprapatellar and popliteal cysts is a clinically pathogenic condition[26]. Crnković mentioned that the suprapatellar cyst developed in the embryonic stage as a separate synovial lesion[26]. The suprapatellar cyst perforates and communicates with the patellofemoral compartment in the fifth month of fetal life[26]. Although we could not observe a clear septum between the suprapatellar cyst and the FPC, the finding of active cavity formation may support the results of the report and lead to better understanding of formation of suprapatellar and popliteal cysts.

In the current study, formation of the medial condyle and mFPC preceded that of the lateral portion. In humans, development of the medial condyle precedes that of the lateral condyle[27], but it remains unknown whether or not the mFPC precedes the lFPC. In adult humans, the structure of the knee joint is asymmetric[27, 28]. This asymmetry is clinically important as it influences the mechanism, capability, and also disease of the knee joint; even bilateral variation of the knee joint is the lowest in the human body[29]. For example, asymmetry of the trochlear groove influences patellar tracking. The patella starts from a slight lateral tilt and then tilts medially until 40°of flexion, laterally until 100°of flexion, then sharply medially beyond 100° of flexion[30]. This abnormal tracking induces osteoarthritis of the patellofemoral joint. Although the structure of the knee joint is different between mice and humans, surgical traumatic osteoarthritis models in mice have been recognized as useful for human osteoarthritis models[30-33].

In summary, the spatial and temporal process of knee joint cavity formation in rat embryos between E14 and E20 was described with 3D reconstructions. Cavitation began from five separate portions at E17, and proceeded asymmetrically. All cavities were connected at E20 when cavitations around the ACL and PCL were completed. The EFIC system had advantages in the present 3D analysis. These results will contribute to a better understanding of

the structural feature and pathology of the knee joint.

Conclusion

Cavity formation initiated from six portions. In each portion, development proceeded asymmetrically. These results concerning anatomic development of the knee joint using EFIC will contribute to a better understanding of the structural feature of the knee joint.

Acknowledgments

The authors thank Rune Fujioka, Akira Ito, Junichi Tajino, Momoko Nagai, Shoki Yamaguchi, Hirotaka Iijima, and Hiroshi Kuroki for their skilled technical assistance and advice.

Author Contributions

Ryota Takaishi performed the experiments, interpreted the data, and drafted the manuscript. Tomoki Aoyama provided financial support, designed the study, and drafted the manuscript. Xiangkai Zhang performed the experiments and interpreted the data. Shinya Higuchi performed the experiments and interpreted the data. Shigehito Yamada provided financial support and technical guidance. Tetsuya Takakuwa provided financial support and final approval of the manuscript to be submitted.

Role of the Funding Source

This study was supported by grants #22591199, #24119002, #25461642, and #23300199 from the Japan Society for the Promotion of Science and BIRD of the Japan Science and Technology Agency.

Conflict of Interest Statement

There are no conflicts of interest.

Figure Legends

Figure 1. Episcopic fluorescence image capture (EFIC) and corresponding histologic section with hematoxylin and eosin staining

A: Representative sagittal section of the knee joint at embryonic day (E) 20, captured using EFIC (i), and corresponding histologic section with hematoxylin and eosin (H&E) staining (ii). Major components of the knee joint were recognizable on both EFIC image and histologic section. The cross section of the posterior cruciate ligament is shown as an area of high intensity (*). Magnification ×50. Resolution = 2.11 μm^2/pixel. Bar = 100 μm.

Abbreviations: F, femur; FPC, femoropatellar cavity; mFMC, medial femoromeniscal cavity; MM, medial meniscus; mMTC, medial meniscotibial cavity; P, patella; T, tibia.

B: Sagittal section of the knee joint at E17, captured using EFIC (i), and corresponding histologic section with H&E staining (ii). The arrow represents the cavity, while the arrowhead represents the border of the cavity. Magnification ×100. Resolution = 1.06 μm^2/pixel. Bar = 100 μm.

C: Sagittal section of the knee joint at E20, captured using EFIC (i), and corresponding histologic section with H&E staining (ii). The arrow represents the cavity, while the arrowhead represents the border of cavity. The anlage of the meniscus is shown as an area of high intensity (*). Magnification ×200. Resolution = 1.06 μm^2/pixel. Bar = 100 μm.

Figure 2. Episcopic fluorescence image capture (EFIC) at embryonic day (E) 16

Representative sagittal section of the right knee joint at E16 (i), and higher magnification (ii). Chondrification of the femur (F), tibia (T), and fibula (not shown) can be observed. A three-layered structure can be seen between the femur and tibia, indicating the interzone (IZ). Magnification ×25. Resolution = 4.22 μm^2/pixel. Bar = 100 μm.

Figure 3. Episcopic fluorescence image capture (EFIC) at embryonic day (E) 17

A: Representative lateral (i), intermediate (ii), and medial (iii) sagittal sections of the right knee joint at E17. Magnification ×60. Resolution = 1.75 μm^2/pixel. Bar = 100 μm.

Abbreviations: ACL, anterior cruciate ligament; F, femur; Fi, fibula; FPC, femoropatellar cavity; lFMC, lateral femoromeniscal cavity; LM, lateral meniscus; mFMC, medial femoromeniscal cavity; MM, medial meniscus; P, patella; PCL, posterior cruciate ligament; T, tibia.

B: Three-dimensional reconstruction of the right knee joint at E17.

White, femur; green, femoropatellar cavity; purple, lateral and medial femoromeniscal cavities.

Figure 4. Episcopic fluorescence image capture (EFIC) at embryonic day (E) 18

A: Representative lateral (i), intermediate (ii), and medial (iii) sagittal sections of the right knee joint at E18. Magnification ×50. Resolution = 2.11 μm^2/pixel. Bar = 100 μm.

Abbreviations: ACL, anterior cruciate ligament; CLC, circumligament cavity; F, femur; Fi, fibula; FPC, femoropatellar cavity; LM, lateral meniscus; mFMC, medial femoromeniscal cavity; T, tibia.

B: Three-dimensional reconstruction of the right knee joint at E18.

White, femur; green, femoropatellar cavity; purple, lateral and medial femoromeniscal and circumligament cavities.

Figure 5. Episcopic fluorescence image capture (EFIC) at embryonic day (E) 19

A: Representative lateral (i), intermediate (ii), and medial (iii) sagittal sections of the

right knee joint at E19. Magnification ×45. Resolution = 2.34 μm^2/pixel. Bar = 100 μm.
Abbreviations: ACL, anterior cruciate ligament; CLC, circumligament cavity; F, femur; Fi, fibula; FPC, femoropatellar cavity; lFMC, lateral femoromeniscal cavity; LM, lateral meniscus; lMTC, lateral meniscotibial cavity; mFMC, medial femoromeniscal cavity; MM, medial meniscus; mMTC, medial meniscotibial cavity; PCL, posterior cruciate ligament; T, tibia.
B: Three-dimensional reconstruction of the right knee joint at E19
White, femur; green, femoropatellar cavity; purple, lateral and medial femoromeniscal, lateral and medial meniscotibial, and circumligament cavities.

Figure 6. Episcopic fluorescence image capture (EFIC) at embryonic day (E) 20

A: Representative lateral (i), intermediate (ii), and medial (iii) sagittal sections of the right knee joint at E20. Magnification ×50. Resolution = 2.11 μm^2/pixel. Bar = 100 μm.
Abbreviations: ACL, anterior cruciate ligament; CLC, circumligament cavity; F, femur; Fi, fibula; FPC, femoropatellar cavity; lFMC, lateral femoromeniscal cavity; LM, lateral meniscus; lMTC, lateral meniscotibial cavity; mFMC, medial femoromeniscal cavity; MM, medial meniscus; mMTC, medial meniscotibial cavity; P, patella; T, tibia.
B: Three-dimensional reconstruction of the right knee joint at E20. The patella is not fully reconstructed and is seen only partially.
White, femur; green, femoropatellar cavity; purple, lateral and medial femoromeniscal, lateral and medial meniscotibial, and circumligament cavities; orange, patella; light blue, anterior cruciate ligament; blue, posterior cruciate ligament.

Figure 7. Morphometry of cavity formation in each developmental stage

Volume of the FPC (green) and the other five cavities (purple, mFMC, lFMC, mMTC, lMTC, and CLC) at each developmental stage was measured. Values are mean ± 95% confidence interval. Abbreviations: CLC, circumligament cavity; FPC, femoropatellar cavity; lFMC, lateral femoromeniscal cavity; lMTC, lateral meniscotibial cavity; mFMC, medial femoromeniscal cavity; mMTC, medial meniscotibial cavity.

References

1. Kenney RR. **The synovial joints: a review of the literature.** *J Am Osteopath Assoc.* 1966;65(10):1092-7
2. Berumen-Nafarrate E, Leal-Berumen I, Luevano E, Solis FJ, Muñoz-Esteves E. **Synovial tissue and synovial fluid.** *J Knee Surg.* 2002;15(1):46-8
3. Goldring MB, Tsuchimochi K, Ijiri K. **The control of chondrogenesis.** *J Cell Biochem.* 2006;97(1):33-44
4. Dowthwaite GP, Edwards JC, Pitsillides AA. **An essential role for the interaction between hyaluronan and hyaluronan binding proteins during joint development.** *J Histochem Cytochem.* 1998;46(5):641-51
5. Wagner M. **Functional anatomy of the knee joint [in German].** *Orthopade.* 1987;16(2):88-99
6. Ralphs JR, Benjamin M. **The joint capsule: structure, composition, ageing and disease.** *J Anat.* 1994;184(Pt 3):503-9
7. Gray DJ, Gardner E. **Prenatal development of the human knee and superior tibiofibular joints.** *Am J Anat.* 1950;86(2):235-87
8. Ito MM, Kida MY. **Morphological and biochemical re-evaluation of the process of cavitation in the rat knee joint: cellular and cell strata alterations in the interzone.** *J Anat.* 2000;197 Pt 4:659-79
9. Gardner E, O'Rahilly R. **The early development of the knee joint in staged human embryos.** *J Anat.* 1968;102(Pt 2):289-99
10. Weninger WJ, Geyer SH. **Episcopic 3D imaging methods: tools for researching gene function.** *Curr Genomics.* 2008;9(4):282-9
11. Weninger WJ, Meng S, Streicher J, Müller GB. **A new episcopic method for rapid 3-D reconstruction: applications in anatomy and embryology.** *Anat Embryol.* 1998;197(5):341-8
12. Weninger WJ, Mohun T. **Phenotyping transgenic embryos: a rapid 3-D screening method based on episcopic fluorescence image capturing.** *Nat Genet.* 2002;30(1):59-65

13. Mohun TJ, Weninger WJ. **Episcopic three-dimensional imaging of embryos.** *Cold Spring Harb Protoc.* 2012;2012(6):641-6
14. Weninger WJ, Geyer SH, Mohun TJ, Rasskin-Gutman D, Matsui T, Ribeiro I, et al. **High-resolution episcopic microscopy: a rapid technique for high detailed 3D analysis of gene activity in the context of tissue architecture and morphology.** *Anat Embryol.* 2006;211(3):213-21
15. Odgaard A, Andersen K, Melsen F, Gundersen HJ. **A direct method for fast three-dimensional serial reconstruction.** *J Microsc.* 1990;159(Pt 3):335-42
16. Ewald AJ, McBride H, Reddington M, Fraser SE, Kerschmann R. **Surface imaging microscopy, an automated method for visualizing whole embryo samples in three dimensions at high resolution.** *Dev Dyn.* 2002;225:369-75
17. Gerneke DA, Sands GB, Ganesalingam R, Joshi P, Caldwell BJ, Smaill BH, et al. **Surface imaging microscopy using an ultramiller for large volume 3D reconstruction of wax- and resin-embedded tissues.** *Microsc Res Tech.* 2007;70(10):886-94
18. Denk W, Horstmann H. **Serial block-face scanning electron microscopy to reconstruct three-dimensional tissue nanostructure.** *PLoS Biol.* 2004;2(11):e329
19. Weninger WJ, Floro KL, Bennett MB, Withington SL, Preis JI, Barbera JP, et al. **Cited2 is required both for heart morphogenesis and establishment of the left-right axis in mouse development.** *Development.* 2005;132(6):1337-48
20. Rosenthal J, Mangal V, Walker D, Bennett M, Mohun TJ, Lo CW. **Rapid high resolution three dimensional reconstruction of embryos with episcopic fluorescence image capture.** *Birth Defects Res C Embryo Today.* 2004;72(3):213-23
21. Yamada S, Samtani RR, Lee ES, Lockett E, Uwabe C, Shiota K, et al. **Developmental atlas of the early first trimester human embryo.** *Dev Dyn.* 2010;239(6):1585-95

22. Tsuchiya M, Yamada S. **High-resolution histological 3D-imaging: episcopic fluorescence image capture (EFIC) is widely applied for experimental animals.** *Congenital Anomalies.* In press
23. Roddy KA, Prendergast PJ, Murphy P. **Mechanical influences on morphogenesis of the knee joint revealed through morphological, molecular and computational analysis of immobilised embryos.** *PLoS One.* 2011;6(2):e17526
24. Dowthwaite GP, Ward AC, Flannely J, Suswillo RF, Flannery CR, Archer CW, et al. **The effect of mechanical strain on hyaluronan metabolism in embryonic fibrocartilage cells.** *Matrix Biol*. 1999;18(6):523-32
25. Dowthwaite GP, Flannery CR, Flannelly J, Lewthwaite JC, Archer CW, Pitsillides AA. **A mechanism underlying the movement requirement for synovial joint cavitation.** *Matrix Biol.* 2003;22(4):311-22
26. Crnković T, Gašpar D, Ethurović D, Podsednik D, Slišurić F. **New insights about suprapatellar cyst.** *Orthop Rev (Pavia)*. 2012;4(1):e9.
27. Varich LJ, Laor T, Jaramillo D. **Normal maturation of the distal femoral epiphyseal cartilage: age-related changes at MR imaging.** *Radiology.* 2000;214(3):705-9
28. Bindelglass DF, Dorr LD. **Current concepts review: symmetry versus asymmetry in the design of total knee femoral components--an unresolved controversy.** *J Arthroplasty.* 1998;13(8):939-44
29. Plochocki JH. **Bilateral variation in limb articular surface dimensions.** *Am J Hum Biol.* 2004;16(3):328-33
30. Rhoads DD, Noble PC, Reuben JD, Mahoney OM, Tullos HS. **The effect of femoral component position on patellar tracking after total knee arthroplasty.** *Clin Orthop Relat Res.* 1990;(260):43-51
31. Mollenhauer JA, Erdmann S. **Introduction: molecular and biomechanical basis of osteoarthritis.** *Cell Mol Life Sci.* 2002;59(1):3-4

32. Brandt KD. **Animal models of osteoarthritis.** *Biorheology*. 2002;39(1-2):221-35

33. Glasson SS, Blauchet TJ, Morris EA. **The surgical destabilization of the medical meniscus (DMM) model of osteoarthritis in the 129/SvEv mouse.** *Osteoarthritis Cartilage.* 2007;15(9):1061-9

34. Chia WT, Pan RY, Tseng FJ, Chen YW, Feng CK, Lee HS, et al. **Experimental osteoarthritis induced by surgical realignment of the patella in BALB/c mice.** *J Bone Joint Surg Br*. 2010;92(12):1710-6

A

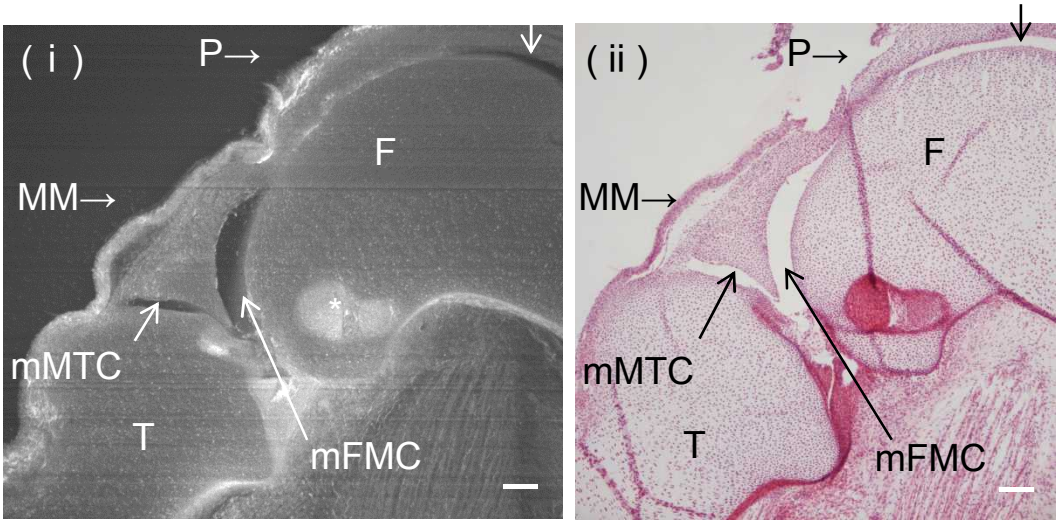

B

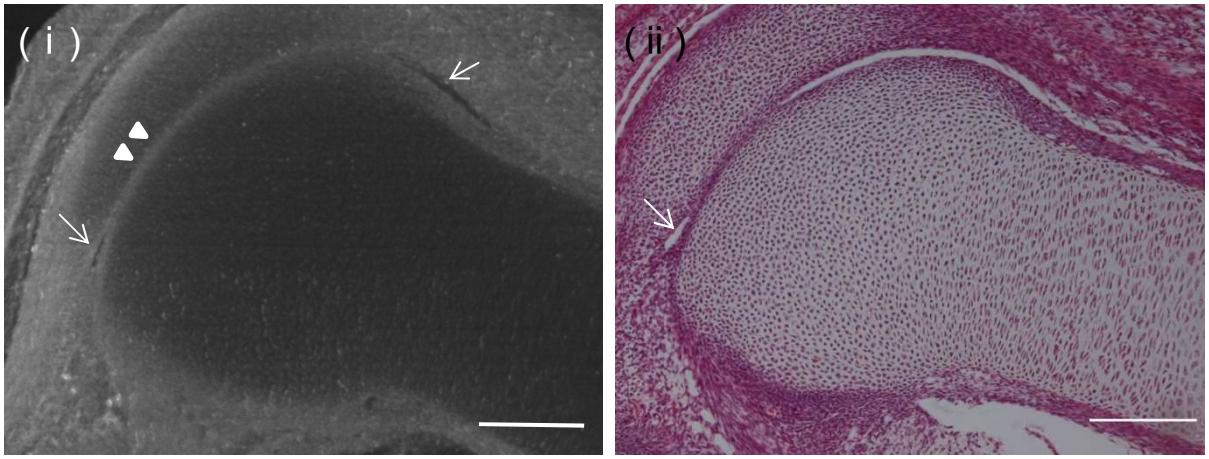

C

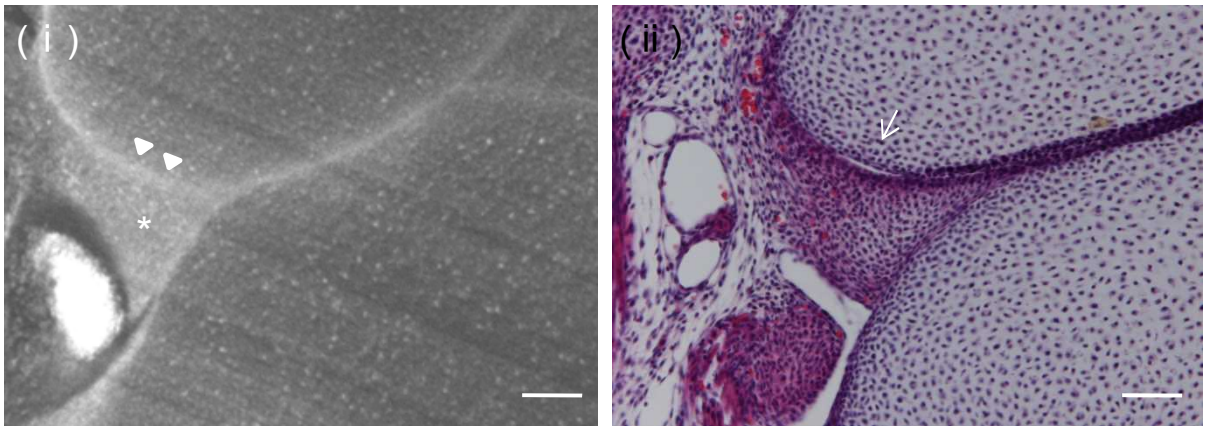

Figure 1

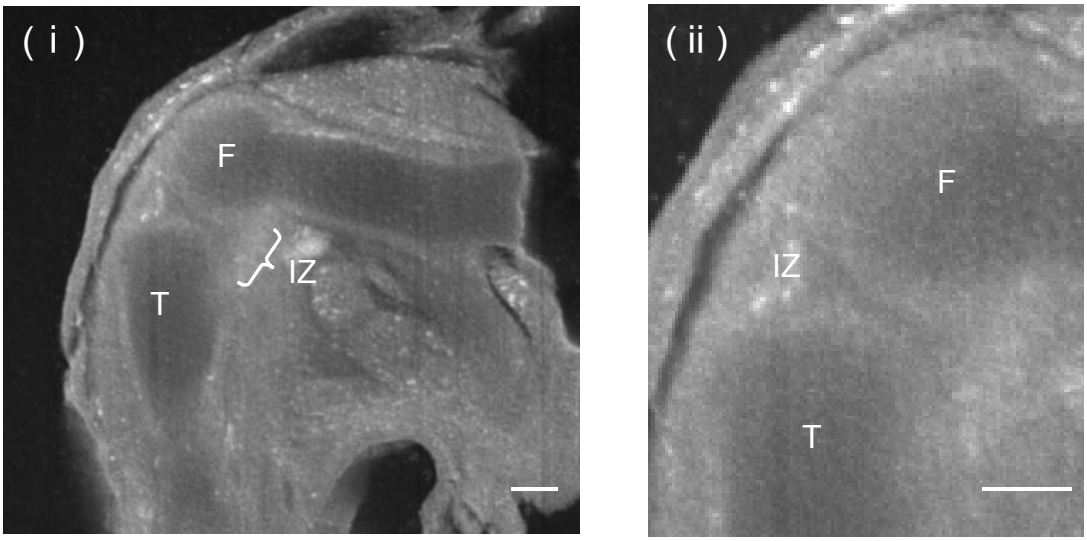

Figure 2

A

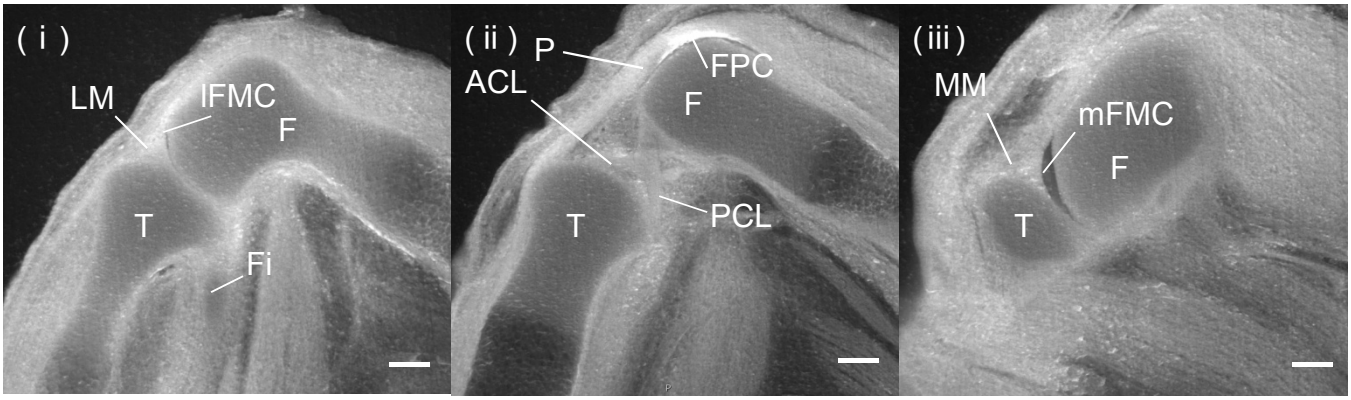

B

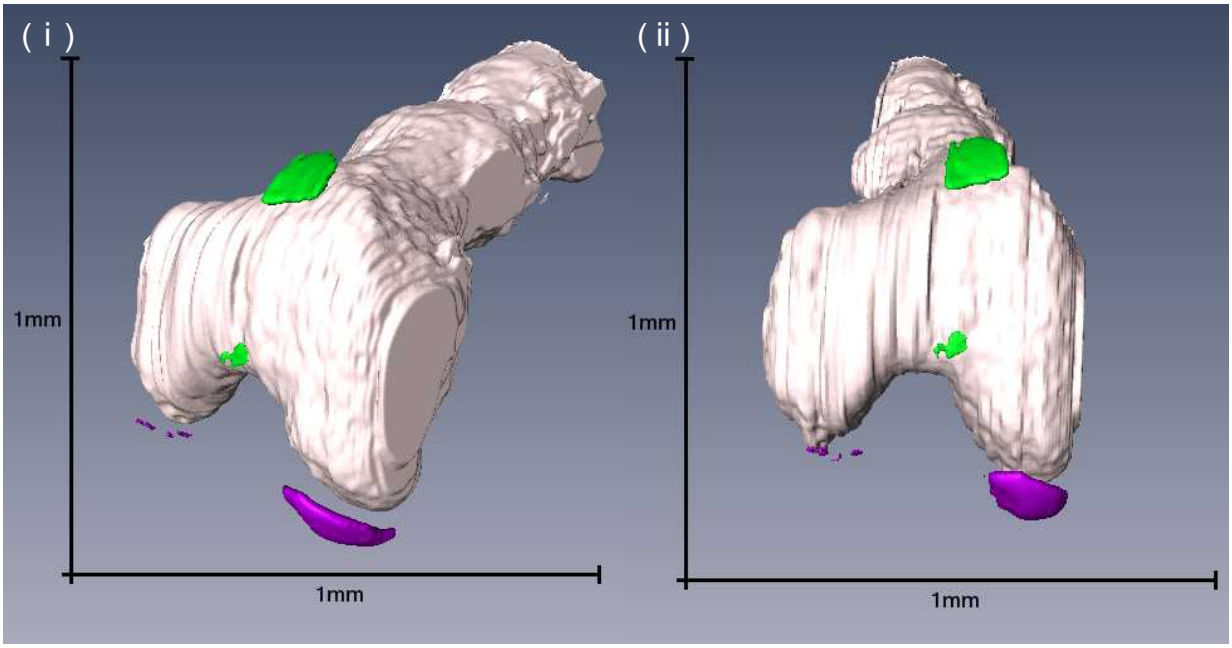

Figure 3

A

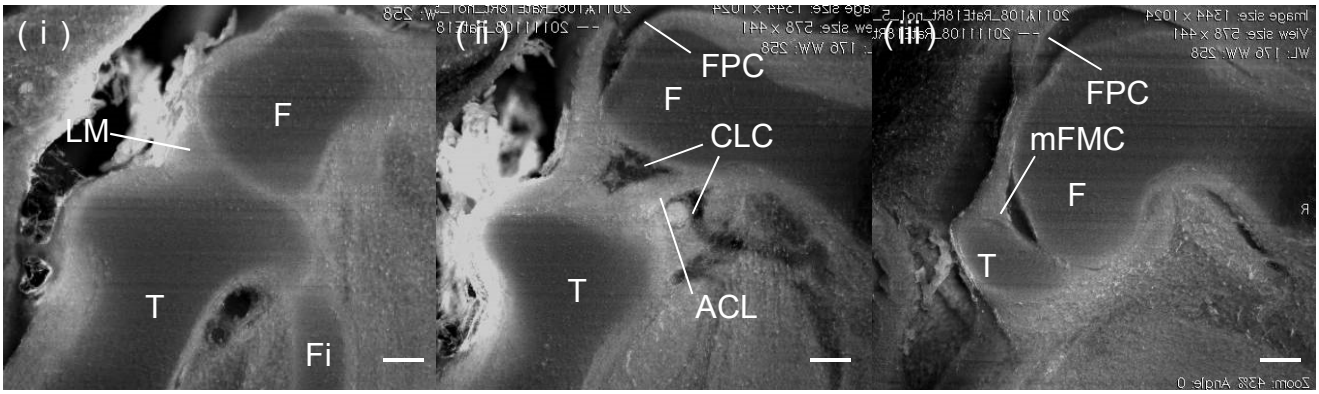

B

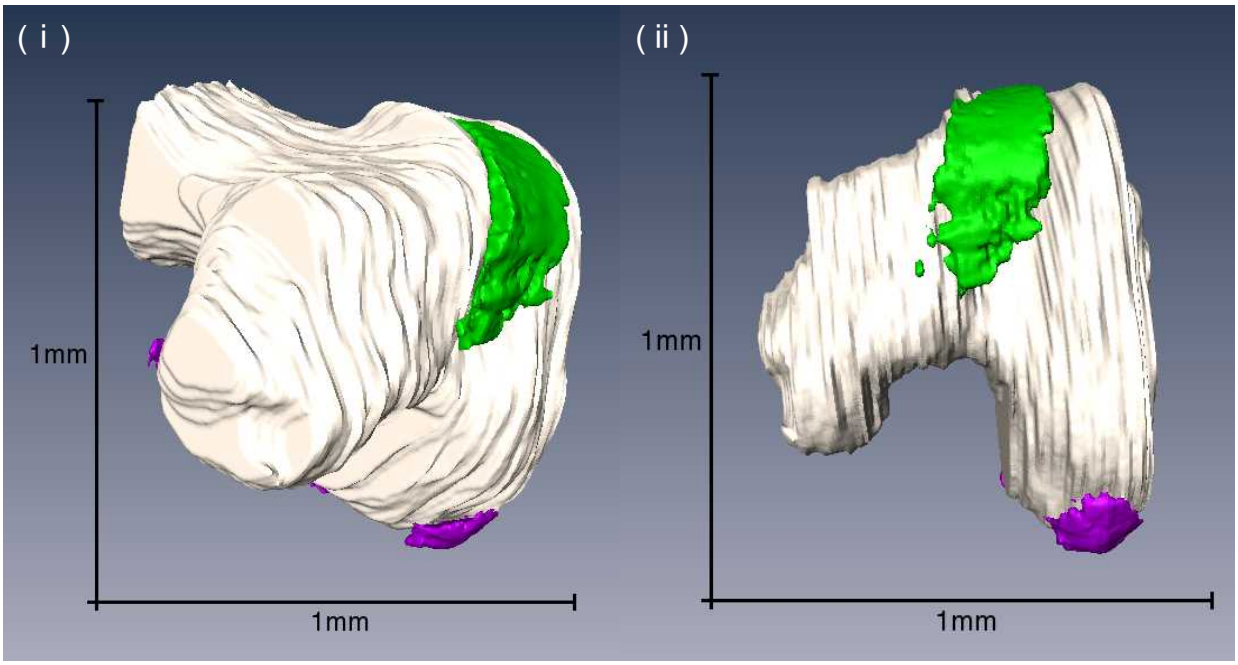

Figure 4

A

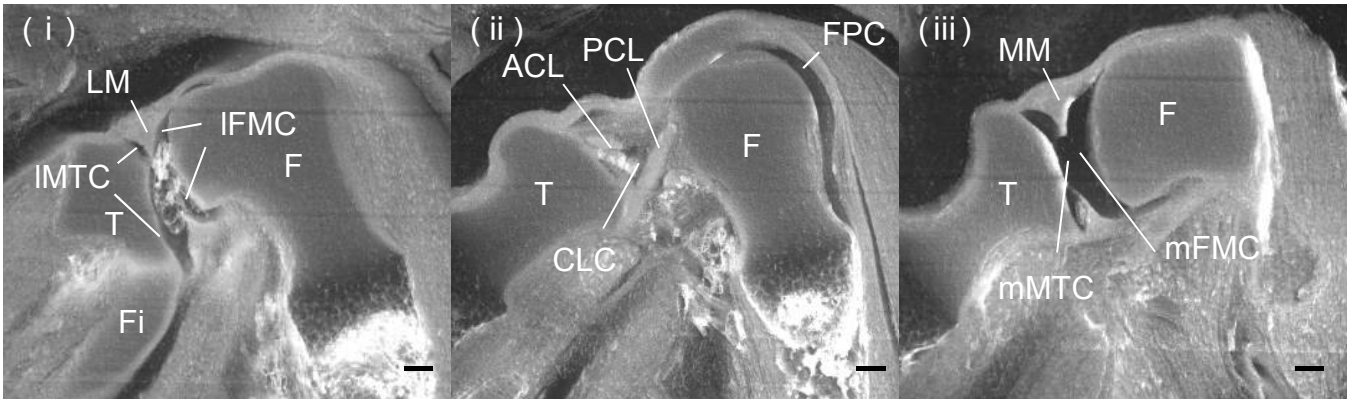

B

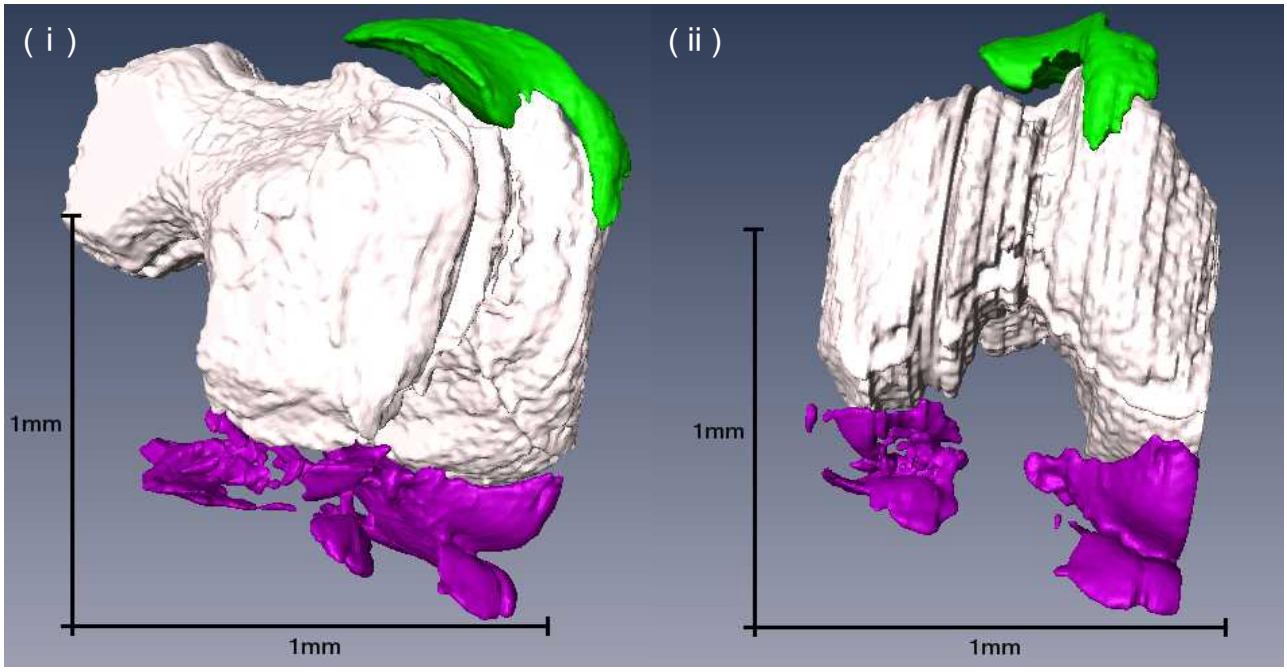

Figure 5

A

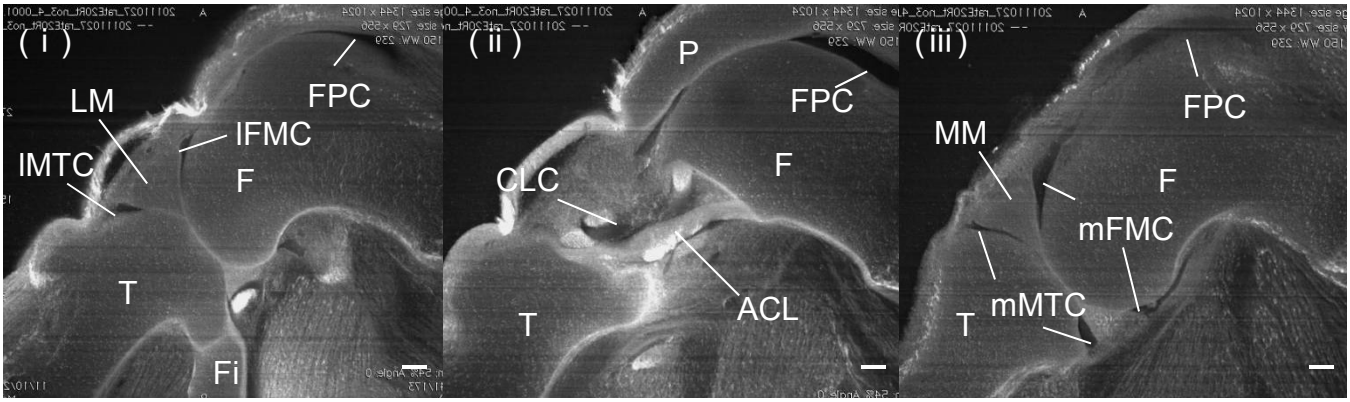

B

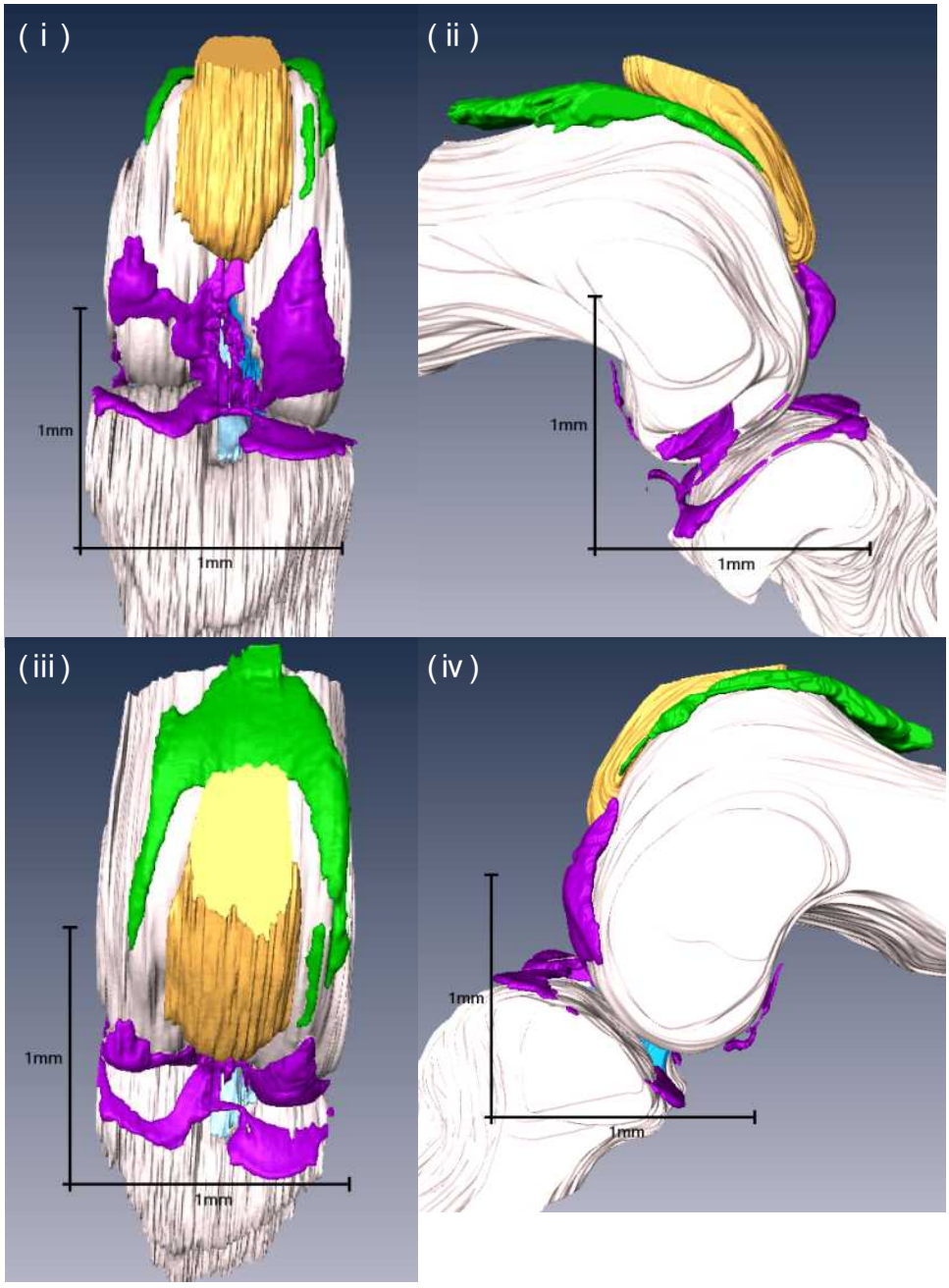

Figure 6

Figure 7